# Experimental study of a vertical plunging jet by means of a volumetric shadowgraph technique

# Experimental study of a vertical plunging jet by means of a volumetric shadowgraph technique

**F Di Nunno[1,2], F Alves Pereira[1], M Miozzi[1], F Granata[2], R Gargano[2], G de Marinis[2] and F Di Felice[1]**

[1] Institute of Marine Engineering, National Council of Research, Rome, Italy
[2] Department of Civil and Mechanical Engineering, University of Cassino and Southern Lazio, Cassino, Italy

fabio.dinunno@unicas.it

**Abstract**. A vertical plunging jet has been investigated experimentally by means of an innovative volumetric shadowgraphy technique. A space carving algorithm has been used for the measurement of the size and concentration of the air bubbles, to follow the air bubbles path inside the investigated volume, providing both spatial and temporal evolution of the same. Furthermore, the air bubble tracking has been performed by means of an algorithm based on the Lucas-Kanade optical flow algorithm. Results highlighted a distribution of the air bubbles that follows the free jet spread inside the investigated volume with a dependence of speed and size from the action exerted by the vertical jet. The volumetric shadowgraph technique has proven effective in characterizing air bubbles, also in presence of relevant void fraction.

## 1. Introduction

The plunging of a falling water jet into a water pool involves the entrainment of a large amount of air bubbles at the impinging point, leading to a submerged air-water flow. Air entrainment phenomena occur in a wide range of situations. Examples in Chemical Engineering are the air-water oxygen transfer through plunging jet entrainment mechanism [1]. In Civil Engineering, air entrainment by plunging jet is a key factor for the proper design and operation of hydraulic structure [2, 3, 4, 5]. A several number of experimental studies on plunging jet are reported in literature, both conducted by means of intrusive conductive probes, which allows to measure air concentration and bubble velocities based on the air-water electrical resistivity difference [6, 7, 8], and non-intrusive optical measurement technique, e.g. Particle Image Velocimetry (PIV), providing the flow field of the two phases and a measurement of the air bubble size and shape [9, 10, 11, 12]. However, for the analysis of air-water flows characterized by high void fraction and/or a strongly three-dimensional dynamic, the investigated region should be extended from a section to a volume.

In this work, an experimental investigation on a vertical plunging jet has been performed by means of a volumetric shadowgraphy technique, providing a characterization of the air bubbles, both in terms of void fraction and geometric features. The measure of the size, shape and concentration of the air bubbles is provided by means of a novel space carving algorithm. Furthermore, the air bubble tracking is evaluated by means of an algorithm based on the Lucas-Kanade optical flow method [13, 14]. A number of experimental results are presented in order to show the suitability of the developed technique for performing a detailed analysis of the air bubbles for two-phase air-water flows in presence of relevant void fraction.

## 2. Materials and Methods

### *2.1. Experimental setup and instrumentation*

The laboratory model consists of a vertical steel pipe (diameter $D$ = 21 mm), from which a water jet comes out and plunges into a squared plexiglas tank (side equal to 14$D$ and height equal to 24$D$) filled with water up to a height of 15$D$. The water level is kept constant by means of a gate valve located downstream of the tank, with a jet falling height $h_f$ of 5$D$. Furthermore, the centreline of the jet is in line with the center of the tank, at 7$D$ from the sidewall. The recirculation of the water in a closed loop is allowed through a centrifugal pump (maximum flow rate equal to 40 l/min). The measurement volume extends from the free surface to 6.5$D$ streamwise (x-direction), from -2.5$D$ to 2.5$D$ spanwise (y-direction) and from -1$D$ to 1$D$ depthwise (z-direction).

The measurement instrumentation consists of four gray-scale cameras equipped with 35 mm focal length lenses, with maximum resolution 1400 x 1024 pixels at 100 fps (frames per second). However, a preliminary analysis of the bubble motion in the vertical plunging jet revealed that the optimal frame rate, that allows the optimal bubble tracking with displacement lower than 10 pixels for velocity of about 1 m/s, is equal to 130 fps, achieved through an active lines reduction, from 1024 to 800. However, the arrangement of the cameras in a vertical position allows the investigation of the jet zone, losing only the most extreme portions of the lateral recirculation zones, the latter characterized by a low void fraction. Cameras are arranged in couples, located in front of two tank sides. The backlight illumination is provided by two LED panels with a dimension of 29,7 cm x 21 cm and a power of 30 W, placed on the opposite side of the tank with respect to the camera couples (Figure 1).

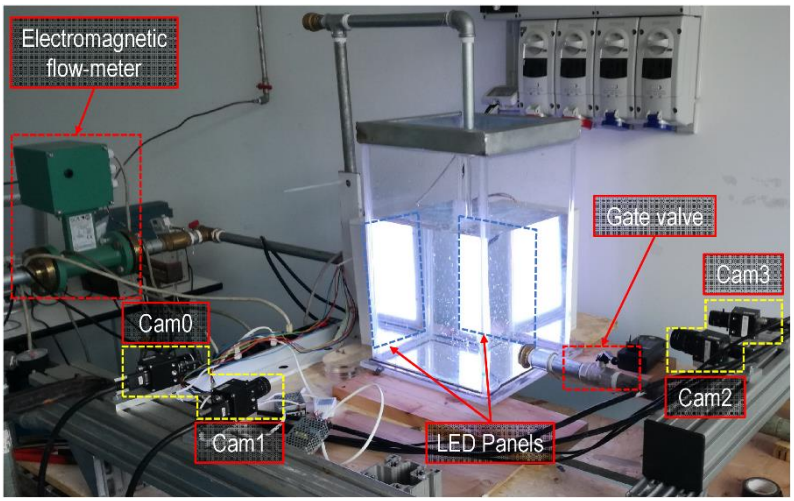


**Figure 1.** Experimental setup.

### *2.2. Measurement technique*

The principle of the used volumetric shadowgraphy technique is the evaluation of the three dimensional position, flow motion and geometrical features of the air bubbles, based on the observation of the air bubble silhouettes from multiple points of view. In particular, the projections of the air bubble silhouette in the Euclidean space, starting from the $n$ points of view, leads to an intersection of $n$ cones, having as apex the optical center of the digital camera lens, with a common finite volume that envelops the identified object. Figure 2 illustrates this principle through the case of an object projection on two planes, with the projection planes indicated as Oxy and O'x'y', with O and O' as optical center and the z-axis as optical axis.

The use of this technique requires a proper calibration step, in order to evaluate the camera parameters: extrinsic, intrinsic and distortion coefficients. Through these parameters it is possible to correct images from lens distortion, convert the image from pixel to world units allowing a measure of the recorded objects and evaluate the camera location with respect to the investigated volume [15]. The estimation of the camera parameters takes place through a calibration procedure that involves the use of specific target

that consists of a planar chessboard (90mm x 50mm) with checkerboard size of 5 mm. The complete calibration procedure is described in detail in Di Nunno et al. (2020) and led to an error in the reprojection of the checkerboard corners in the 3D space between −1.5 pixels to 1.5 pixels corresponding to −0.2 mm to 0.2 mm. In addition, the technique has been validated through a series of measurements on polypropylene spheres of known size [16].

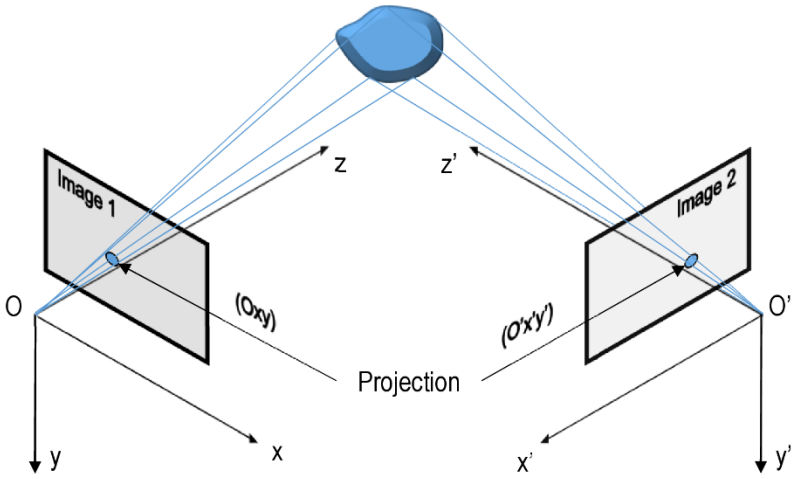


**Figure 2.** Measurement principle.

*2.3. Image processing*

In a shadowgraphy image containing air bubbles, the image background presents the highest pixel intensity while the bubbles show the lowest one. In Figure 3 are represented the image processing algorithm for the bubble silhouettes detection, applied simultaneously on the sets of images recorded from each camera. The first operation is the background removal (Figure 3b), obtained by subtracting the median image from the entire set of images (Figure 3a). Images are then binarized using the IsoData algorithm (Figure 3c, [17]). Since the bubbly flows with significant air concentrations characterized by the presence of bubble clusters, the detection of the single bubbles inside clusters is improved using the watershed technique. This technique considers the cluster as hydrographic basins adjacent to each other, allowing their division and, consequently, their detection (Figure 3d, [18, 19]). Finally, the detection of the bubble silhouettes is obtained by considering the outline pixel of the air bubbles (Figure 3e).

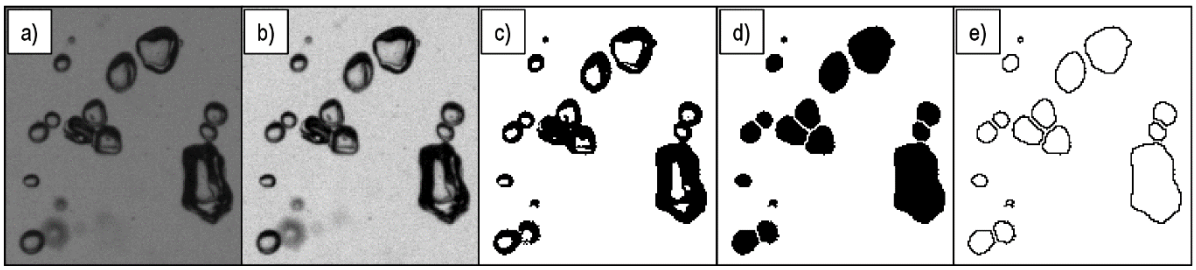


**Figure 3.** Steps for the silhouettes detection: raw image (a); background removal (b); binarization (c); watershed (d); detection of the bubble silhouettes (e).

## 3. Results and Discussion

An experimental campaign has been conducted, consisting of three data sets, recorded increasing the water flow rate $Q_w$, from the minimum flow rate for the air bubble entrainment inception, that occurs for a water flow rate equal to 0.5 l/s (PJ1), passing from 0.6 l/s (PJ2), until 0.7 l/s (PJ3). An increase in water flow rate, passing from PJ1 to PJ2 and PJ3, corresponds to a non-linear growth of the air entrained, as can be observed in Figure 4 and better explained in the subsequent results. The number of frames for each data set is equal to 2000, recorded at 130 fps.

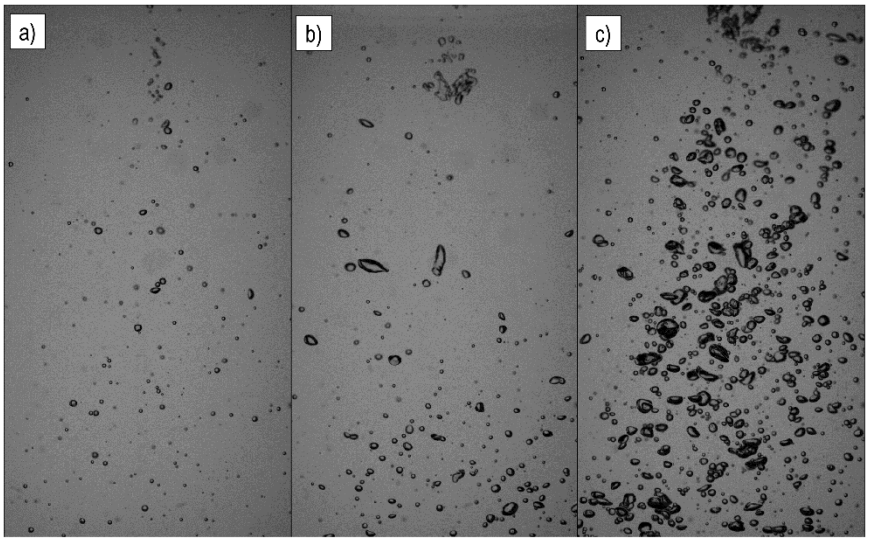


**Figure 4.** Recorded images: PJ1 (a); PJ2 (b); PJ3 (c).

A statistical analysis of the air bubble geometric features and velocity for the three data sets has been conducted. The voxel presents a side of 2 mm. The maximum number of air bubbles for each voxel is equal to: 221 (PJ1), 275 (PJ2) and 496 (PJ3). Figure 5 shows the dimensionless void fraction, expressed as the ratio between the void fraction $\Phi_b$ and the relative maximum value $\Phi_{b,max}$, the latter equal to 3.25% for PJ1, 5.10% for PJ2 and 14.86% for PJ3, with the void fraction calculated as:

$$\phi_b = \frac{N_b}{N_f} \cdot \frac{V_b}{V_v} \tag{1}$$

where number of detected bubbles $N_b$, $N_f$ is the number of recorded frame, equal to 2000 for the three data sets, $V_b$ is the mean volume of the air bubble equivalent sphere inside the voxel with volume $V_v$. The distribution follows the free jet spread inside the investigated volume. For the three data sets, the ratio $\Phi_b/\Phi_{b,max}$ is equal to or exceeds 80% inside the jet zone while it is close to 30% inside the recirculation zones.

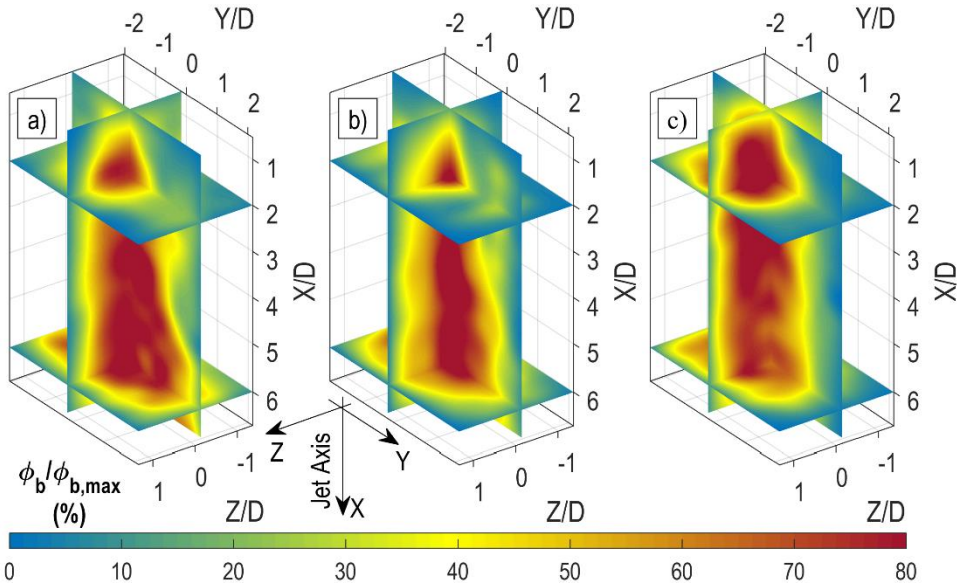


**Figure 5.** Dimensionless void fraction: PJ1 (a); PJ2 (b); PJ3 (c).

The air bubble size has been measured and expressed in terms of air bubble equivalent diameter. Figure 6 reports the horizontal profiles of the mean equivalent diameter in the plane $Z/D = 0$, highlighting peaks inside the recirculation zones with lower values in the jet zone. The size of the air bubbles inside the jet zone is affected by the action exerted by the vertical plunging jet. When the same reach the lateral recirculation zones, the air bubble rising is governed exclusively by the buoyancy forces, involving an increase of size, which becomes more marked as the depth decreases, owing to the simultaneous reduction of the water pressure on the bubble surface.
The air bubble tracking in the Euclidean space has been also performed starting from the bubble boundaries in the 2D frames recorded from each camera. Considering the volumetric shadowgraphy application here used, a 2D vector field has been obtained, where each vector indicates the displacement of a point of the bubble silhouettes between the consecutive frames. Knowing the bubble positions in the Euclidean space, it is possible to interpolate a 3D vector field, based on the *n* 2D vector fields related to the *n* cameras. Figure 7 shows the streamwise velocity for the three data sets. As the depth from the free surface increases, passing from $X/D = 2$ to $X/D = 6$, the bubbles tend to rise owing to the buoyancy force, which counteracts the forces exerted by the liquid jet on the same. Therefore, the jet zone is characterized by positive streamwise velocities, from top to bottom, while negative streamwise velocities are observed inside the lateral recirculation zone.

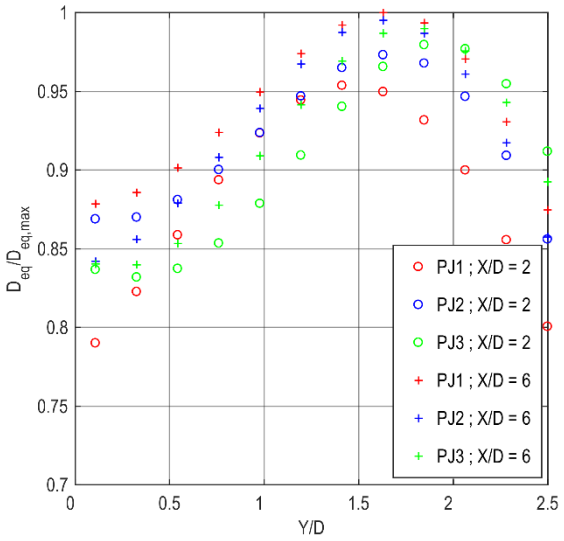


**Figure 6.** Air bubble: equivalent diameter (Plane $Z/D = 0$).

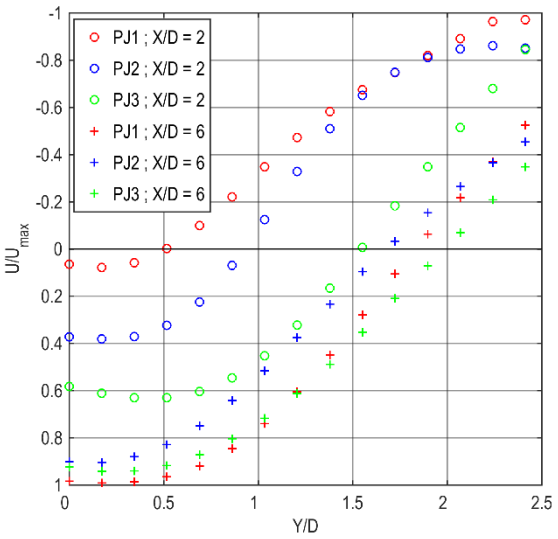


**Figure 7.** Air bubble mean streamwise velocity profiles (Plane $Z/D = 0$).

## 4. Conclusions

An experimental investigation on a vertical plunging jet has been presented. In order to allow a three-dimensional analysis of the air bubbles, a volumetric shadowgraphy technique has been used, which allows to follow the trajectories of the air bubbles inside the investigated volume, providing a measurement of the size and concentration of the air bubbles.
Results show an air bubble distribution that follows the free jet spread inside the investigated volume. The size of the air bubbles is affected by the action of the plunging jet. Along the lateral recirculation zones, the rising depends exclusively from the buoyancy forces, with an increase of size as the depth decreases, owing to the simultaneous reduction of the water pressure on the bubble surface. In addition, the air bubble tracking shows positive streamwise velocities, from top to bottom, inside the jet zone with negative one along the lateral recirculation zone. Overall, the technique has proved to be well-suited for an accurate analysis of the air bubbles in a two-phase air-water flow, also in presence of relevant void fraction.

**Acknowledgments**
This work was partially conducted under the support of the Italian Ministry of Education, University and Research 2017 PRIN Project ACE, grant 2017 RSH3JY. The activities were also partially conducted under Grant CTN01_00176_163601, "Technology and Industrial Research for Marine Mobility - TRIM", coordinated by the National Research Council of Italy, co-funded by the Ministry of Education, University and Research.

**5. References**

[1] Kumar M Ranjan S T N and Gupta R 2017 Plunging hollow jet aerators - oxygen transfer and modeling *ISH J. Hydraul. Eng.* **24**(1) pp 61-67
[2] Granata F de Marinis G Gargano R and Tricarico C 2013 Novel approach for side weirs in supercritical flow *J. Irrig. Drain. Eng.* **139**(8) pp 672-679.
[3] Granata F de Marinis G and Gargano R 2015 Air-water flows in circular drop manholes *Urban Water J.* **12**(6) pp 477-487.
[4] Granata F 2016 Dropshaft cascades in urban drainage systems *Water Sci. Technol.* **73**(9) pp 2052-2059.
[5] Granata F and de Marinis G 2017 Machine learning methods for wastewater hydraulics *Flow Meas. Instrum.* **57** pp 1-9.
[6] Sene K 1988 Air entrainment by plunging jets *Chem. Eng. Sci.* **43**(10) pp 2615-2623
[7] Chanson H Aoki S and Hoque A 2004 Physical modelling and similitude of air bubble entrainment at vertical circular plunging jets *Chem. Eng. Sci.* **59** pp 747-758
[8] Xu W Chen C and Wei W 2018 Experimental Study on the Air Concentration Distribution of Aerated Jet Flows in a Plunge Pool Water, **10**(12) p 1779
[9] Hammad K 2010 Liquid Jet Impingement on a Free Liquid Surface: PIV Study of the Turbulent Bubbly Two-Phase Flow *Proc. ASME 3rd Joint, FEDSM* **1** pp 2877-2885
[10] Kendil F Z Danciu D V Schmidt M Salah A B Lucas D Krepper E and Mataoui A 2012 Flow field assessment under a plunging liquid jet *Prog. Nucl. Energy* **56** pp 100-110
[11] Harbya K Chivab S and Muñoz-Coboa J 2014 An experimental study on bubble entrainment and flow characteristics of vertical plunging water jets *Exp. Therm. Fluid. Sci.* **57** pp 207-220
[12] Di Nunno F Alves Pereira F de Marinis G Di Felice F Gargano R Granata F and Miozzi M 2019 Two-phase PIV-LIF measurements in a submerged bubbly water jet *J. Hydraul. Eng.* **145**(9)
[13] Lucas B and Kanade T 1981 An Image Registration Technique with an Application to Stereo Vision *Proc. IUW* pp 121-130
[14] Miozzi M Jacob B and Olivieri A 2008 Performances of feature tracking in turbulent boundary layer investigation *Exp. Fluids* **45**(4) pp 765-780.
[15] Trucco E and Verri A 1998 Introductory Techniques for 3-D Computer Vision *Prentice Hall*
[16] Di Nunno F Alves Pereira F Granata F de Marinis G Di Felice F Gargano R and Miozzi M 2020 A shadowgraphy approach for the 3D Lagrangian description of bubbly flows *Meas. Sci. Technol.* under review
[17] Ridler T and Calvard S 1978 Picture thresholding using an iterative selection method *IEEE T. Syst. Man. Cy. S.* **SMC-8** pp 630-632.
[18] Vincent L and Soille P 1991 Watersheds in digital spaces: an efficient algorithm based on immersion simulations *IEEE T. Pattern Anal.* **13**(6) pp 583-598.
[19] Di Nunno F Alves Pereira F de Marinis G Di Felice F Gargano R Granata F and Miozzi M 2018 Experimental study of air-water two-phase jet: Bubble size distribution and velocity measurements *J. Phys. Conf. Ser.* **1110**.